Journal Name

ARTICLE TYPE

Cite this: DOI: 10.1039/xxxxxxxxxx

Dynamic self-assembly of microscale rotors and swimmers†

Megan S. Davies Wykes,*[a] Jérémie Palacci,[b,a,‡] Takuji Adachi,[c] Leif Ristroph,[a] Xiao Zhong,[c] Michael D. Ward,[c] Jun Zhang,[a,d,e] and Michael J. Shelley[a]

Received Date
Accepted Date

DOI: 10.1039/xxxxxxxxxx

www.rsc.org/journalname

Biological systems often involve the self-assembly of basic components into complex and functioning structures. Artificial systems that mimic such processes can provide a well-controlled setting to explore the principles involved and also synthesize useful micromachines. Our experiments show that immotile, but active, components self-assemble into two types of structure that exhibit the fundamental forms of motility: translation and rotation. Specifically, micron-scale metallic rods are designed to induce extensile surface flows in the presence of a chemical fuel; these rods interact with each other and pair up to form either a swimmer or a rotor. Such pairs can transition reversibly between these two configurations, leading to kinetics reminiscent of bacterial run-and-tumble motion.

Self-assembly is a hallmark of biological systems as organisms construct functional complex materials and structures from simpler components. The use of self-assembly in the fabrication of new materials is attractive owing to its inherent versatility and potential for mass production[1]. Research has focused primarily on systems where the formation of macrostructures does not require the continuous input of energy[2–5], a process known as equilibrium self-assembly. Another route to self-assembly is dynamic: where structures persist only while energy is being supplied to the system[6]. Artificial micron-scale motors, immersed in a fuel laden fluid, have been shown to spontaneously self-organize into crystal structures[7], and form into asters of two or more particles[8]. These studies have active components, producing a local fluid flow which leads to motility. A striking aspect of these active systems is their potential for emergent dynamics, whereby individuals and groups have qualitatively different behaviour[9], such as flocking[10], formation of flow structures on larger scales than the individual components[11], or collective flows which are faster than those induced by individual active particles[12].

Here we describe how two of the simplest machines can be formed by dynamic self-assembly from a single type of building block. Active, but immotile, rods spontaneously self-assemble into structures that exhibit the two fundamental types of motion: rotation and translation (Fig. 1). This occurs without imposing any external field. Assemblies can transition between rotor and swimmer, leading to behaviour reminiscent of the run-and-tumble motion of *E. coli*[13]. The type and direction of motion is determined by the configuration of rods in an assembly, thereby linking the self-assembly to the emergent motility. This is a rare example of artificial dynamic self-assembly and therefore represents an important step towards making more complex micron-scale machines.

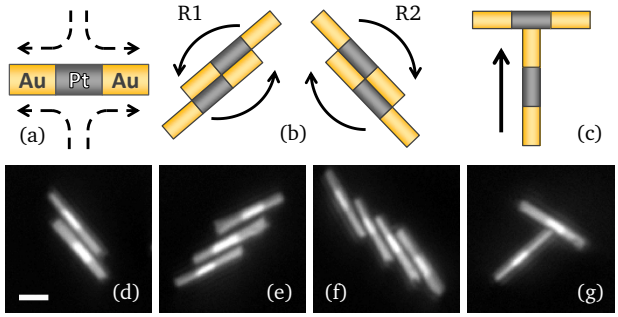

Fig. 1 (a) Schematic of tripartite rod and expected extensional flow. Motion of (b) rotors in arrangement R1 and R2, (c) T-swimmers (vertical rod is the leg, horizontal rod is the top). Micrographs of (d-f) rotors, (g) T-swimmer. Scale bar 1μm refers to all micrographs.

1 System and phenomenology

The particles described herein are constructed of three metal sections, in the arrangement gold-platinum-gold (Au-Pt-Au). These micron-scale rods are expected to produce an extensile flow when submerged in a solution of chemical fuel (Fig. 1a). These parti-

[a] *Applied Mathematics Laboratory, Courant Institute, New York University; Email: megan.davies wykes@nyu.edu*
[b] *Department of Physics, UC San Diego; E-mail: palacci@physics.ucsd.edu*
[c] *Molecular Design Institute, Department of Chemistry, New York University.*
[d] *Department of Physics, New York University.*
[e] *NYU-ECNU Institutes of Mathematical Sciences and Physics Research, NYU-Shanghai.*
† Electronic Supplementary Information (ESI) available: [details of any supplementary information available should be included here]. See DOI: 10.1039/b000000x/

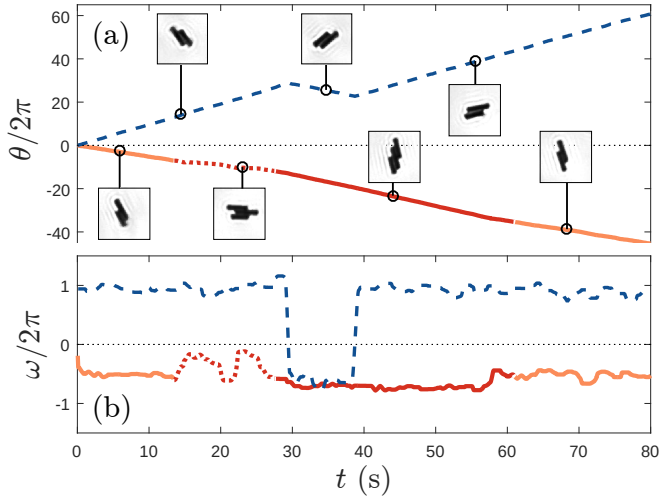

Fig. 2 Rotor which changes direction (blue, dashed) and a rotor that has a rod added to it (red, orange): the rotor begins with two rods (orange), separates and re-forms with three rods (red). The three-rod assembly is initially in a staggered arrangement (red, dotted), then adjusts to become a three-rod rotor (red, solid), then loses a rod, becoming a two-rod rotor (orange). Plotted are (a) the total number of rotations $\theta/2\pi$ (winding number), (b) the rotation rate, $\omega/2\pi$ (Hz). Counter-clockwise is positive.

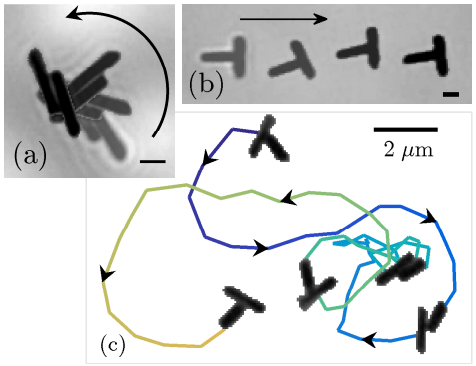

Fig. 3 Overlay images of (a) rotor, time interval: 0.5 s, (b) T-swimmer, time interval: 1 s. Scale bars 1μm. (c) Path taken by a pair of rods transitioning from T-swimmer, to rotor, to T-swimmer (scale bar refers to path, overlay images at $\frac{1}{2}$ scale). Overlay images at $t = 0$, 1.6, 4.4, 5, and 7.2 seconds.

cles are 'active' in that they generate a flow, but are immotile as this flow is symmetric and asymmetric motion is required to swim at low Reynolds number. Although many studies have examined self-assembly for motile particles, there have been few experimental studies on the self-assembly of active, but immotile particles. A very recent report by Jewell *et al.*, submitted to this journal nearly simultaneously with this article, demonstrated that tripartite rods made from ruthenium and gold segments (in the arrangements Ru-Au-Ru and Au-Ru-Au) could self-assemble into various configurations[14]. The report by Jewell, *et al.* does not describe the motility of these particles, and is complementary to the results described herein. Experiments of silver nanorods surrounded by contractile flows (the reverse of those studied here), induced by an external electric field that also aligns the nanorods, have found evidence of hydrodynamic pair interactions[15]. Theoretical studies of 'extensors' have indicated the presence of interesting collective behaviour[16,17]. In the case of individually immotile particles, motility itself can be a signature of emergent dynamics as it indicates some form of symmetry breaking in the system.

The system described here builds on research into micron-scale bipartite gold-platinum (Au-Pt) rods, which swim by self-electrophoresis when placed in a solution of hydrogen peroxide (H_2O_2) fuel[18–24]. Electrochemical decomposition of H_2O_2 results in a gradient in proton concentration, which corresponds to an electric field pointing from Pt to Au[25]. The rods themselves have an overall negative charge. Therefore, the positively charged electrical double layer surrounding the rod experiences a force due to the self-generated electrical field[24–26]. A fluid flow develops on the rod surface, from Pt to Au, causing the rod to swim with its Pt end leading. Swimming rods have been observed to form pairs transiently[27], suggesting the presence of attractive interactions. The composition of particles can be tailored, thereby altering the flow configuration around a rod.

Tripartite rods of length $2.18 \pm 0.4\mu$m and diameter $0.34 \pm 0.08\mu$m are fabricated as described in the Supplementary Information (SI; see Fig. 1a). The motion of these particles on a glass coverslip is observed using an inverted optical microscope, with a $100\times$ objective (oil immersion, N.A. 1.4) and diascopic illumination. The particles are dense compared to the solution and in experiments they settle and are essentially confined to 2D motions along the lower surface of the chamber. There will be a hydrodynamic interaction between the rod and the wall. Although models exist for this interaction, it is still an open area of research[20,28,29]. Our previous study of bipartite metallic rods argued, using lubrication theory, for a hydrodynamic attraction between motile active rods and walls[20]. Reflected illumination can be used to identify the individual metal segments (Fig. 1d-g). When these tripartite rods are placed in a solution of H_2O_2 they spontaneously self-assemble into several distinct configurations (Fig. 1b-g).

The attraction between rods appears short-ranged, on the order of a rod length, as further separated rods appear to act diffusively. The most common assembly consists of two or more parallel and regularly staggered rods, as seen in Figs. 1d-f and 3a. Rotors were most commonly composed of two or three rods, but up to seven rod rotors were also observed (see SI Fig. 1d). Stable rotors assembled from more than two rods nearly always show a staircase arrangement. An example of rotor self-assembly is included as supplementary movie S1. Once assembled, these structures rotate at a steady rate and in a direction determined by the rod configuration (Fig. 1b and 2). As the rods are dense compared to the solution, they are essentially confined to 2D and consequently rotor geometries are chiral. There are two observed arrangements, referred to as R1 and R2, as illustrated by Fig. 1b. Rotors always rotate with the outer rod leading, i.e. R1 rotates counter-clockwise and R2 rotates clockwise. Individual rotors have mean rotation rates in the range $\omega = 0.4 - 2$Hz for 3% H_2O_2 (SI). While some rotors breakup after short times (~ 10s), others persist without breakup for longer than the recording time of experiments (> 120s) and are sufficiently stable to survive col-

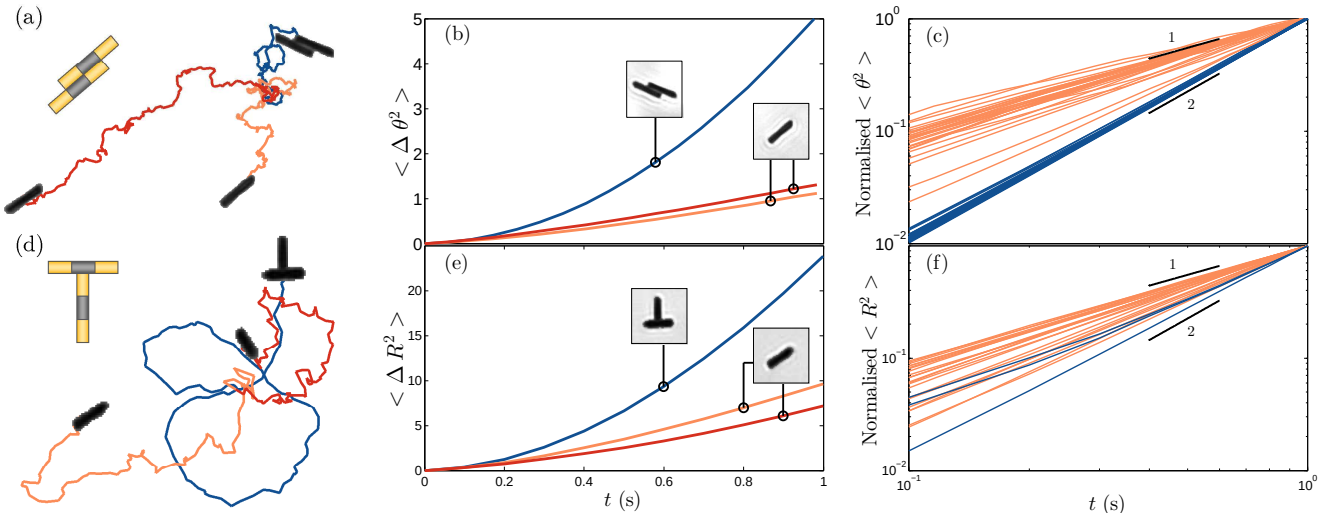

Fig. 4 Dynamics of a rotor and a T-swimmer: (a) Tracks of rotor (blue) and component rods after breakup (orange, red) plotted for 10s. (b) MSAD (rad^2/s^2) for rotors and rods from (a). (c) MSAD (normalised by maximum value) for 40 rotors (blue) and 29 single rods (orange). (d) Tracks of T-swimmer (blue) and component rods after breakup (orange, red) plotted for 10s. (e) MSD (μm^2/s^2) for T-swimmer and rods from (d). (f) MSD (normalised by maximum value) against time for 3 T-swimmers (blue) and 33 single rods (orange). The majority of single rods have slightly super-diffusive translation and rotation, consistent with slight motility. Rotor MSAD shows a quadratic dependence on time, characteristic of powered rotation. T-swimmers show a mix of translational diffusion and powered translation. Overlaid micrographs on (a,d) are to scale with particle tracks.

lisions with other rods.

Assembly is generally reversible – pairs can separate and reform – and the reassembled structures rotate at an identical speed and in the same direction, if reassembled in the original configuration. In Fig. 2a (dashed line) an example is shown where a rotor begins in configuration R1, rotating counter-clockwise (defined as positive). At 30s, thermal fluctuations cause the rods within a rotor to break apart. When the rotor reforms, it has switched to configuration R2 and starts rotating in a clockwise direction. At 40s, the rotor breaks apart a second time, returning to the original R1 configuration and again rotating counter-clockwise. The rotation speed of this example is plotted in Fig. 2b (dashed line) and is equal to 1 Hz when rotating counter-clockwise and 0.5 Hz when rotating clockwise. Many rotors rotate at identical speeds even after a change of direction. An example of a rotor changing direction is included as movie S2. Rods can be added to existing rotors, creating yet larger rotating aggregates (Fig. 1e,f). When a rod is added to a rotor this results in a small change in rotation rate. An example of this is shown in Fig. 2, where a rotor initially composed of two rods (orange) has a rod added to it (red). Initially the three-rod assembly is in a staggered arrangement (red, dotted), but then adjusts to become a three-rod rotor (red, solid). At a later time, the assembly separates back to a two-rod rotor (orange). An example of a rod being added to a rotor is included as movie S3. The staggered arrangement that appears as an intermediary state is less common than the staircase arrangements seen in rotors.

Another self-assembled structure is the T-swimmer, consisting of two perpendicular rods joined by a Pt-Au junction, which swims in a direction aligned with the leg of the 'T', towards the end with the junction (Fig. 1c and Fig. 3b). An example can be seen in movie S4. This shape is much less common than the rotors, accounting for only $\sim 5\%$ of assemblies. T-swimmers persist for shorter times than rotors ($\sim$ 10s) and are often a transitional state when a rotor reverses direction or otherwise breaks alignment (as in movie S2). When a rotor and a T-swimmer collide a variety of events can happen. The rotor tends to stay a rotor, but the rods that make up the T-swimmer can become part of the rotor, or continue as a T-swimmer, or become a separate rotor, or break apart to become single rods. All of these have been observed and a movie illustrating the interactions of T-swimmers with rotors is included as supplementary movie S6. Interestingly, pairs can transition repeatedly between the T-swimmer and rotor configurations. As a T-swimmer, the pair swims in looping trajectories, as seen in Fig. 4d, while a rotor essentially spins in place. Figure 3c shows the trajectory of a particle pair that starts as a T-swimmer, transitions into a rotor, and then returns to the T-swimmer configuration (see movie S5). Switching between the two states is most likely a result of thermal fluctuations, which is consistent with the time spent either as a rotor or a swimmer being apparently randomly distributed. Rotation for a random length of time will cause the swimming direction to be randomised when the pair switches back to a T-swimmer. These characteristics make the dynamics of a particle pair that is persistently switching between states reminiscent of bacterial run-and-tumble behaviour.

2 Analysing the emergent dynamics

We have stated that individual rods appear to act diffusively and assemblies show motility. In the following section we use a model to demonstrate the change in behaviour between single rods and assemblies. We model the dynamics using overdamped Langevin equations for the path (x,y) and angle θ of particle[30,31]:

$$\frac{\mathrm{d}x(t)}{\mathrm{d}t} = v\cos(\theta(t)) + \sqrt{2D}\xi_x(t), \qquad (1)$$

$$\frac{dy(t)}{dt} = v\sin(\theta(t)) + \sqrt{2D}\xi_y(t), \tag{2}$$

$$\frac{d\theta(t)}{dt} = \omega + \sqrt{2D_r}\eta(t). \tag{3}$$

Here v is the speed of the particle, ω is its rotation rate in rad/s, D is the translational diffusion coefficient and D_r is the rotational diffusion coefficient. The noise terms ξ_x, ξ_y and η are uncorrelated Gaussian processes with zero mean and unit variance[31,32]. We have approximated the diffusion of rods and assembled structures as isotropic[23,33], which is sufficient to demonstrate the difference in behaviour between single rods and assemblies, although descriptions that include the effects of anisotropic diffusion have also been studied[34–36].

Equation (3) is decoupled from Eqs. (1,2) and can be integrated to give the mean-squared angular displacement (MSAD)

$$\left\langle \Delta\theta(t)^2 \right\rangle = \omega^2 t^2 + 2D_r t \tag{4}$$

where $\Delta\theta(t)^2 = (\theta(t_0+t) - \theta(t_0))^2$ and $\langle\bullet\rangle$ indicates an average over a time series. Equation (4) shows that deterministic rotation results in a quadratic MSAD, whereas rotational diffusion results in a linear MSAD[31–33].

The tracks of a rotor (blue) and the component rods after breakup (red, orange) are each plotted for 10s in Fig. 4a. The MSAD reveals the fundamentally different dynamics of a pair compared to a single rod (Fig. 4b). The rotation of individual rods is diffusive, but when assembled into a rotor the MSAD is quadratic with time, characteristic of deterministic rotation. The MSAD for several rotors and single rods are plotted in Fig. 4c. The motion of rotors is dominated by deterministic rotation, while the motion of the majority of single rods is diffusive.

Solving Eqs. (1-3) to find the mean-squared displacement (MSD) reveals the existence of several regimes[33]. For $t \ll 1/D_r$ and $t \ll 1/\omega$, the MSD takes the limiting form of

$$\left\langle \Delta R(t)^2 \right\rangle = 4Dt + v^2 t^2 \tag{5}$$

showing that locomotion results in a MSD that is quadratic in time[30]. The trajectories of a T-swimmer and its component rods are each plotted for 10s in Fig. 4d. The MSD shows dramatically enhanced swimming when the rods are assembled into a T-swimmer (Fig. 4e). Comparing the MSD for several single rods and T-swimmers (Fig. 4f), it appears that individual rods have a spectrum of behaviours: many are diffusive, but some are swimming, which could be due to asymmetries in the rods. The nearly quadratic MSD of T-swimmers indicates a component of deterministic translation, while the change in gradient of in Fig. 4f shows that the deterministic component $4Dt$ is of a similar magnitude to v^2t^2 for this time.

Fitting Eq. (4) to the MSAD allows the measurement of ω and D_r, while fitting the solution of Eqs. (1-3) to the MSD allows the measurement of v and D [33]. Estimates of D_r are in agreement with previous work[37]. An effective long-time diffusion coefficient

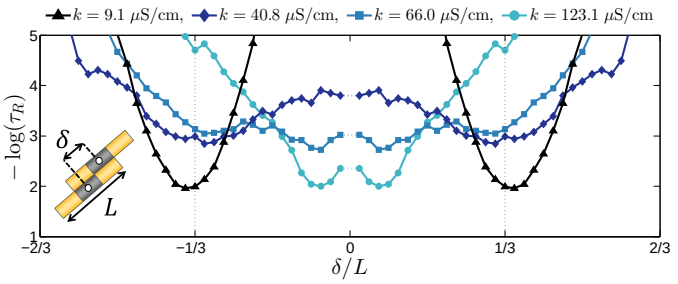

Fig. 5 The pseudopotential $-\log(\tau_R)$ as a function of rotor offset δ/L , where τ_R is the fractional residence time or probability of an offset. An offset of $\delta \approx L/3$ (see inset) is most prevalent at the lowest conductivity, which corresponds to no added salt. Adding salt increases conductivity, k, and leads to a broader distribution of offsets. As only the magnitude of δ is measured, $-\log(\tau_R)$ is reflected about $\delta = 0$.

can be calculated analytically from Eqs. (1-3), as

$$D_{\text{eff}} = D + \frac{v^2 D_r}{2(D_r^2 + \omega^2)}, \tag{6}$$

indicating an enhanced diffusivity from motility, with this enhancement lessened by rotation[33]. Interestingly, measured rotor values of D_{eff} are in general smaller than those measured for single rods without fuel and decreases with the number of rods in a rotor. This might be expected as rotors are longer than single rods, which reduces D [37]. The smaller D_{eff} does not indicate that $v = 0$, as the enhancement of the translational diffusion is reduced by rotation and is negligible if $9v^2 \ll 2L^2(D_r^2 + \omega^2)$ [37]. In fact, rotors move in circular orbits, indicating that $v \neq 0$. The distribution of radii of these orbits is of the same order of magnitude as the distribution of rod lengths, suggesting that the non-zero v is due to variations in the rods.

3 Self-assembly

The assembly of rods may be influenced by many physical effects, including hydrodynamic, electric, thermal and steric interactions. For the extensile rods studied here, simulations indicate that hydrodynamics alone is sufficient to bring together pairs of parallel rods[17]. To examine the effect of the flow surrounding the rod, experiments were conducted using rods of the alternative configuration, Pt-Au-Pt (not shown). These particles are expected to generate a contractile flow, the reverse of Fig. 1a. Parallel pairs were not observed to form. This suggests that hydrodynamic attraction is important for bringing the rods into maximal proximity, revealing the importance of the design of the rods for the self-assembly.

The detailed configuration of assemblies is influenced by additional effects. In particular, rotors exhibit a measurable and robust offset between the centres of the constituent rods, as seen in Fig. 1d-f. This observation is quantified by examining the magnitude of the offset δ between the centroids of paired rods in a rotor (Fig. 5, inset) and measuring its variation in time. The fractional residence time τ_R is the time spent at a particular offset as a proportion of the total time of an experiment. We plot $-\log(\tau_R)$ in Fig. 5 as, in an analogy with an equilibrium system, the energy

of a state $E(\delta) \sim -\log(\tau_R)$. The black curve reveals a minimum centred at $\delta \approx L/3$, giving a preferred overlap that places the Pt and Au segments of each rod into close proximity. This suggests that electro-kinetic effects play an important role in determining the configuration. Simulations by Jewell *et al.* suggest that the 1/3 offset minimizes the electrostatic repulsion between the rods that make up a rotor[14].

These observations suggest that self-assembly is driven by both hydrodynamic and electro-kinetic interactions, which together compete against thermal effects. Changing the conductivity of the solution by the addition of sodium chloride salt (NaCl), weakens both the electro-kinetic and hydrodynamic interactions, thus varying the relative importance of these effects. Specifically, changing the conductivity exerts three main effects: (i) The electric field strength E in the solution has an inverse relationship with conductivity k by Ohm's law, $E = i/k$, where i is the ion flux[38]; (ii) The swimming speed of bipartite swimmers has an inverse relationship to solution conductivity $U \sim 1/k$, where U is the swimming speed[39] and a similar relationship for the flow around the tripartite rods would be expected; (iii) The length scale λ of the near-surface region where flow and electric field occur, scales as $\lambda \sim 1/k$.

Due to the weakened interactions, it is expected that the offset between rods will be more widely distributed. Experiments were conducted at 5% H_2O_2 and four values of the conductivity (corresponding to NaCl concentrations of 0, 0.17, 0.44, and 0.87 mM), again measuring the variation in the magnitude of δ, here by examining the change in overall perimeter of a rotor over time (SI). The results are plotted as pseudopotentials in Fig. 5, where the black curve corresponds to no added salt. Increasing the conductivity results in the component rods sliding parallel to each other, causing large variations in δ over time and thus a more uniformly distributed pseudopotential. At high conductivities, an offset of zero is most energetically favourable. The simulations of Jewell *et al.* show that this totally overlapped state is hydro-dynamically favourable[14].

4 Discussion

The formation of both rotors and T-swimmers from symmetric active particles has also been reported in a computational simulations of filaments constructed of active beads producing force-free, torque-free flows in a fluid, confined to move in 2D in an infinite domain[17]. Filaments surrounded by an overall extensile flow (globally similar to what is expected for the rods studied here) formed into parallel pairs which rotate, but in the opposite direction to that which is observed in our experiments (i.e. in these simulations R1 would rotate clockwise, R2 counter-clockwise). The formation of T-swimmers was also predicted by these simulations, but for component filaments surrounded by contractile flows[17]. In contrast, the T-swimmers in our experiments were formed from rods inducing extensile flows in their surroundings and ordered assemblies were not observed to form in experiments using rods with contractile flows.

The motion of rotors and T-swimmers might be explained by considering the extensile outer fluid flows that are created by these structures. In the case of rotors, the combination of the offset between the rods and the extensile outer flow fields would result in rotation in the observed direction. Likewise, the net result of the extensile outer flows around a T-swimmer is to pump fluid against and from the top of a T-swimmer down the leg, causing the T-swimmer to swim with the top leading, as observed. This is a general argument that would predict the observed motion for offset rotors and T-swimmers, assembled from any rods which are surrounded by extensile flows, so long as the outer flow is left essentially unchanged when the rods assemble into rotors and T-swimmers. The possibility of an additional mechanism for the motion of rotors and T-swimmers exists for these tripartite Au-Pt-Au particles, as there is the potential for electrical interactions between adjacent rods. If the overlapped Pt and Au segments of rods within a rotor can pump fluid from Pt to Au, then a rotor can be conceived as two anti-parallel swimmers, and would result in the observed rotation. Similarly, an electrically induced flow across the Pt-Au junction in the T-swimmer would explain its direction of motion. Either or both of these mechanisms would explain the observed motion.

We have described the dynamic and reversible self-assembly of rotors and T-swimmers from symmetric, tripartite Au-Pt-Au micron-scale rods. Self-assembly breaks the symmetry of individual particles, leading to directed motion. In the case of rotors, the symmetry is broken because of a misalignment of the rods, presumably due to the electrical interactions, as quantified by the energy landscape of Fig. 5. This system has rich dynamics, resulting from the complex interplay of various forces, with the potential for control over the rotation rate, swimming velocity and lifetime of assembled structures through the fuel concentration, solution conductivity and tailoring of particle geometry and composition. This is a rare example of artificial dynamic self-assembly, a process common in nature. Systems of this type are of interest not only because of potential applications in micro-fluidics but also because a more detailed understanding of dynamic self-assembly could lead to insights about similar processes in nature.

5 Acknowledgements

We thank Marjorie Lopez, of the University of Puerto Rico, for playing a key role in setting up the process for synthesizing nanorods at the Department of Chemistry, New York University, as part of the REU program. We also thank Y. Liu, A. Hollingsworth and M. Driscoll for useful conversations. This work was primarily supported by the Materials Research Science and Engineering Center (MRSEC) program of the National Science Foundation under Award Number DMR-1420073. M.S.D.W. thanks the Fulbright Scholarship Lloyds of London Award for financial support. T.A. thanks the JSPS Postdoctoral Fellowships for Research Abroad for the financial support. This article is based on work presented at the APS/DFD meeting in 2015, in session L39.00008 "Dynamic self-assembly of microscale rotors and swimmers."

References

1 G. M. Whitesides and B. Grzybowski, *Science*, 2002, **295**, 2418–2422.

2 J. Zhang, E. Luijten and S. Granick, *Annual Review of Physical Chemistry*, 2014, **66**, 581–600.

3 S. Sacanna, W. T. M. Irvine, P. M. Chaikin and D. Pine, *Nature*, 2010, **464**, 575–578.

4 Q. Chen, S. C. Bae and S. Granick, *Nature*, 2011, **469**, 381–384.

5 Y. Wang, Y. Wang, D. R. Breed, V. N. Manoharan, L. Feng, A. D. Hollingsworth, M. Weck and D. Pine, *Nature*, 2012, **490**, 51–55.

6 W. Wang, W. Duan, S. Ahmed, A. Sen and T. E. Mallouk, *Accounts of Chemical Research*, 2015, **48**, 1938–1946.

7 J. Palacci, S. Sacanna, A. P. Steinberg, D. Pine and P. M. Chaikin, *Science*, 2013, **339**, 936–340.

8 S. Ahmed, D. T. Gentekos, C. A. Fink, T. E. Mallouk and A. E. T. Al, *ACS nano*, 2014, **8**, 11053–11060.

9 D. Saintillan and M. J. Shelley, *Comptes Rendus Physique*, 2013, **14**, 497–517.

10 A. Bricard, J.-B. Caussin, N. Desreumaux, O. Dauchot and D. Bartolo, *Nature*, 2013, **503**, 95–98.

11 T. Sanchez, D. T. N. Chen, S. J. DeCamp, M. Heymann and Z. Dogic, *Nature*, 2012, **491**, 431–434.

12 D. Saintillan and M. J. Shelley, *Journal of The Royal Society Interface*, 2012, **9**, 571–585.

13 H. C. Berg and R. M. Berry, *Physics Today*, 2005, **58**, 64–65.

14 E. L. Jewell, W. Wang and T. E. Mallouk, *Soft Matter*, 2016, 2–5.

15 K. a. Rose, B. Hoffman, D. Saintillan, E. S. G. Shaqfeh and J. G. Santiago, *Physical review. E, Statistical, nonlinear, and soft matter physics*, 2009, **79**, 011402.

16 D. Saintillan and M. J. Shelley, *Physical Review Letters*, 2007, **99**, 058102.

17 A. Pandey, P. B. S. Kumar and R. Adhikari, *arXiv: cond-mat.soft*, 2014.

18 W. F. Paxton, K. C. Kistler, C. C. Olmeda, A. Sen, S. K. St. Angelo, Y. Cao, T. E. Mallouk, P. E. Lammert and V. H. Crespi, *Journal of the American Chemical Society*, 2004, **126**, 13424–13431.

19 Y. Wang, R. M. Hernandez, D. J. Bartlett, J. M. Bingham, T. R. Kline, A. Sen and T. E. Mallouk, *Langmuir*, 2006, **22**, 10451–10456.

20 D. Takagi, J. Palacci, A. B. Braunschweig, M. J. Shelley and J. Zhang, *Soft Matter*, 2014, **10**, 1784–1789.

21 Y. Wang, S. T. Fei, Y. M. Byun, P. E. Lammert, V. H. Crespi, A. Sen and T. E. Mallouk, *Journal of the American Chemical Society*, 2009, **131**, 9926–9927.

22 S. J. Ebbens and J. R. Howse, *Soft Matter*, 2010, **6**, 726–738.

23 D. Takagi, A. B. Braunschweig, J. Zhang and M. J. Shelley, *Physical Review Letters*, 2013, **110**, 038301.

24 J. L. Moran, P. M. Wheat and J. D. Posner, *Physical Review E*, 2010, **81**, 065302.

25 W. Wang, T. Y. Chiang, D. Velegol and T. E. Mallouk, *Journal of the American Chemical Society*, 2013, **135**, 10557–10565.

26 J. L. Moran and J. D. Posner, *Journal of Fluid Mechanics*, 2011, **680**, 31–66.

27 W. Wang, W. Duan, A. Sen and T. E. Mallouk, *Proceedings of the National Academy of Sciences of the United States of America*, 2013, **110**, 17744–9.

28 S. E. Spagnolie, G. R. Moreno-Flores, D. Bartolo and E. Lauga, *Soft Matter*, 2015, **11**, 3396–3411.

29 A. P. Berke, L. Turner, H. C. Berg and E. Lauga, *Physical Review Letters*, 2008, **101**, 1–4.

30 J. R. Howse, R. A. L. Jones, A. J. Ryan, T. Gough, R. Vafabakhsh and R. Golestanian, *Physical Review Letters*, 2007, **99**, 048102.

31 S. van Teeffelen and H. Löwen, *Physical Review E*, 2008, **78**, 020101.

32 N. A. Marine, P. M. Wheat, J. Ault and J. D. Posner, *Physical Review E*, 2013, **87**, 052305.

33 S. J. Ebbens, R. A. L. Jones, A. J. Ryan, R. Golestanian and J. R. Howse, *Physical Review E*, 2010, **82**, 015304.

34 Y. Han, A. Alsayed, M. Nobili, J. Zhang, T. C. Lubensky and A. G. Yodh, 2006, **314**, 626–630.

35 B. ten Hagen, S. van Teeffelen and H. Löwen, *Journal of physics. Condensed matter : an Institute of Physics journal*, 2011, **23**, 194119.

36 F. Kümmel, B. Ten Hagen, R. Wittkowski, I. Buttinoni, R. Eichhorn, G. Volpe, H. Löwen and C. Bechinger, *Physical Review Letters*, 2013, **110**, 1–5.

37 M. Doi and S. F. Edwards, *The theory of polymer dynamics*, Oxford University Press, 1986.

38 W. F. Paxton, P. T. Baker, T. R. Kline, Y. Wang, T. E. Mallouk and A. Sen, *Journal of the American Chemical Society*, 2006, **128**, 14881–14888.

39 J. L. Moran and J. D. Posner, *Physics of Fluids*, 2014, **26**, year.